LDACS1 RANGING RESULTS FROM FLIGHT EXPERIMENTS

D. Shutin, N. Schneckenburger, M. Walter, T. Thiasiriphet, N. Franzen, A. Filip, and M. Schnell
German Aerospace Center (DLR), 82234 Wessling, Germany

Abstract

In recent years the German Aerospace Center (DLR) has been actively working on a proposal to deploy an L-band Digital Aeronautical Communication System type 1 (LDACS1) for future Alternative Positioning, Navigation, and Timing (APNT) services. In 2012 a flight measurement campaign has been performed to validate LDACS1-based navigational functionality. The results indicated a strong influence of multipath propagation on ranging performance. To better characterize multipath environment for future ground-based APNT services a second measurement has been performed in November 2013. This paper outlines the November 2013 measurement campaign and provides corresponding range estimation results that make use Bayesian filtering methods and Doppler smoothing to mitigate multipath and improve range estimation.

Introduction

Air-Traffic Management (ATM) modernization as developed under SESAR and NextGen in Europe and the US, respectively, is enabled by future technologies for Communications, Navigation, and Surveillance (CNS). In navigation, further development of the Global Navigation Satellite System (GNSS) as primary means of navigation is ongoing. GNSS with Space Based Augmentation Systems and Ground Based Augmentation Systems will cover not only the en-route airspace in future, but extend its application area towards a seamless gate-to-gate navigation, including approach, landing, take-off, and taxiing even under CAT III conditions. The future availability of multi-frequency, multi-constellation GNSS will greatly assist in improving the robustness of the satellite services. However, in view of the ever-growing dependency of air navigation services on GNSS, ICAO recommended to assess the need and feasibility of an alternative position, navigation and timing (APNT) system, for the situations when the GNSS service is unavailable.

In communications, new data links are developed to assist the ATM modernization process. For air-ground communications the L-band Digital Aeronautical Communication System (LDACS) is currently under development. Recently, LDACS type 1 (LDACS1) [1] – one of the two LDACS proposals for standardization – has been extended to include a navigational functionality to enable future APNT services [2][3][4]. To develop LDACS1-based APNT approach, the German Aerospace Center (DLR) has performed two measurement campaigns in November 2012 [2], [5] and November 2013.

The goal of the first campaign was to implement a core structure of the LDACS1 system for navigation and test its performance in a realistic scenario with an airborne receiver. The analysis of the measurement data collected during the campaign has revealed that multipath propagation has a very strong impact on ranging performance of the system. In order to investigate multipath path propagation in more details, a second measurement campaign has been performed. This paper describes the second measurement campaign, as well as discusses new Doppler-smoothed ranging results for multipath-degraded signals.

Measurement campaign setup

The goals of the second measurement campaign in November 2013 are (i) a detailed analysis and modeling of multipath effects in L-band to assess their impact on ranging performance, and (ii) investigation of LDACS1-ranging in more diverse flight scenarios. In order to achieve the first goal, a relatively wideband sounding signal (10MHz bandwidth) centered at 970MHz was used. The corresponding signal was a peak-to-average power ratio (PAPR) optimized multitone signal [6]. The time period of the transmit signal is 512µs; it also determines both the maximum resolvable Doppler frequency, $f_{D,max} = (2t_{symb})^{-1}$, as well as the maximum range, $r_{max} = t_{symb} \cdot c$, which can be resolved without ambiguities. In the latter expression c denotes the speed of light in air at sea level. For the second goal an LDACS-conform signal was employed, just as in the first measurement campaign.

The parameters of the used signals are summarized in Table 1.

Table 1. Selected parameters of the transmitted signals used in the measurement campaign

Parameter	10MHz	LDACS1
Bandwidth [MHz]	10	0.5
Symbol duration [µs]	512	120
Correlation width [m]	30	600
Range ambiguity [km]	153	-
Max Doppler [Hz]	900	4150

The core of the measurement setup for the used signals remained unchanged (see also Figure 2); it only slightly deviated from the setup used during the first campaign in November 2012 [7]. However, for these measurements only a single transmitter was used, which permits computation of the range to the aircraft but not its position.

At the transmitter side, the setup included a Cs (cesium) atomic clock, a GPS time receiver, an arbitrary waveform signal generator (AWG), and a power amplifier. The GPS time receiver was used to monitor Cs clock drift during the measurements. The AWG was programmed to generate either a passband version of the 10MHz multitone signal for channel sounding, or the corresponding LDACS1-conform signal. The transmitter hardware was located in a van. A mobile transmitter is chosen to be able to travel between the aircraft at the apron and the transmit antenna's location. This is needed for calibrating the measurement setup and accurate synchronization of the transmitter and receiver.

The transmit antenna is setup on top of a building 23m above ground level (AGL) at an altitude of 652m above mean sea level (AMSL). In Figure 1 the area surrounding the transmit antenna, as seen from the antenna's position is shown in a 360° panorama. The chosen location of the transmitting antenna and surrounding infrastructure mimics well a typical small airport environment.

a)

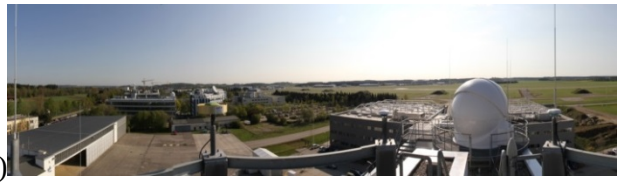

b)

Figure 1. View from the antenna to (a) north and (b) south directions.

As a transmitting antenna we use an L-band aircraft communication blade antenna (Sensor Systems S65-5366-715) with vertical polarization. Before the measurements, the actual antenna position is measured using very accurate GPS carrier phase measurements, providing a centimeter-level accuracy of the estimated antenna position.

The airborne setup included a low noise pre-amplifier, an Rb (rubidium) atomic clock, a programmable receiver implemented on a National Instruments PXIe platform, and a GPS time receiver. The latter served two functions: (i) a monitoring of the Rb clock drift during measurements, and (ii) a computation of the "ground-truth" GPS-based range to the aircraft. The key element in the measurement was an accurate cable-based calibration of the measurement equipment. During the calibration, the transmitter and receiver were connected directly with a cable, and the transmitted signal was recorded. The recorded calibration signal was later used in the processing of the measured signals for range estimation (see also [5] for more details). The calibration was performed twice: before the flight and after the landing. This was done to achieve two goals. First, the calibration signal recorded in this way readily accounts for amplitude and phase dispersions at the processing stage. These distortions can thus be canceled by correlating the received signal with the recorded calibration signal. Second, the phase of the calibration signal also accounts for the offset between the transmitter clock and receiver clock at the calibration time.

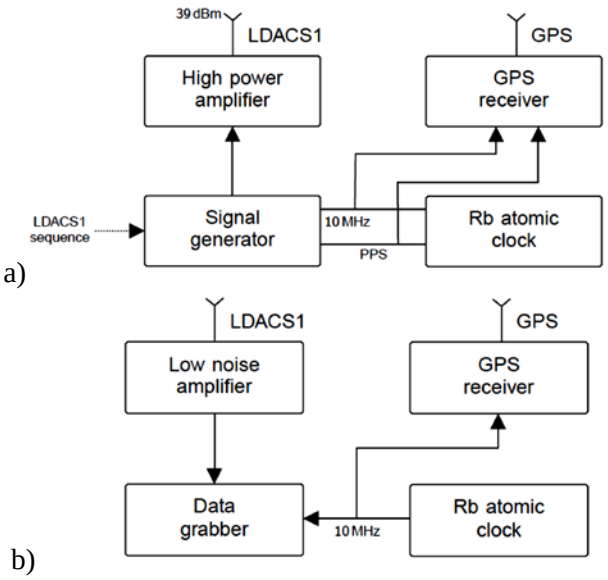

Figure 2. A block diagram representing the key components of the used measurement setup at the (a) transmitter and (b) receiver

Since the drift of both transmitter and receiver atomic clocks with respect to GPS is monitored during the measurements, the exact offset between clocks can thus be recovered at the post-processing stage by setting the clock offset at the calibration time to zero. This permits an estimation of the actual range between the transmitter and receiver and its comparison to the computed GPS range.

DLR's research aircraft D-CMET, a Dassault Falcon 20E, shown in Figure 3, is used as a platform for the airborne receiver. The setup of the on-board hardware was organized in three 19" racks on the right side of the fuselage. Note that the positions of the GPS receiving antenna and LDACS receiving antennas were not collocated. As a result, the estimated LDACS range will deviate from the "ground truth" range obtained based on GPS data from the on-board GPS receiver. These deviations will in general depend on the relative co-location of both antennas with respect to the ground transmitting antenna; specifically, it will depend on the attitude and heading of the aircraft. To be able to correct the difference in the computed ranges, an airplane orientation, i.e., pitch, roll and yaw, has been recorded with 1Hz rate. This allows correcting the GPS-based range and computing the GPS-based

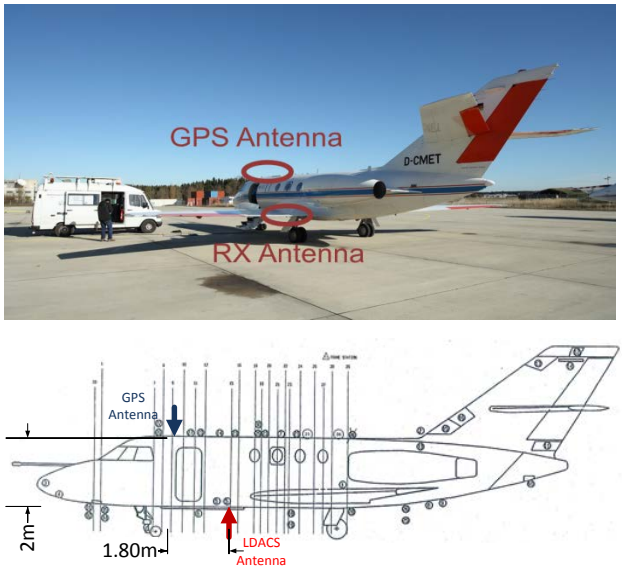

Figure 3. Dassault Falcon 20E airplane used in the measurement campaign with the positions of the receiving GPS and LDACS antennas

position of the LDACS antenna for an accurate comparison of the results.

Flight scenarios

In Figure 4 we show the flown trajectories, as well as GPS ranges and altitudes for the 10MHz-wide signals. In Figure 5 flights with the LDACS1-conform signals are summarized. The trajectories were selected so as to investigate the propagation channels (i.e., with 10MHz signals) in a number of different scenarios and phases of the flight. For LDACS1 signals similar trajectories were flown. An exception was made for the flight 2 with LDACS1 signals (Figure 5b) that was performed with an in-band DME interference at 968MHz. This measurement was possible thanks to a support from the German Air Service Provider (Deutsche Flugsicherung). For the measurement, a test DME, located in Kaufbeuren, Germany, and used for training purposes, was tuned to 968MHz. The LDACS1 signals were then transmitted first 500kHz away from the DME channel (at 968.5MHz), and then 1.5MHz away from the DME channel (at 969.5MHz); such deployment mimics very well the planned in-lay deployment of LDACS1 system in the L-band. During the measurements the airplane flew directly over the DME station at flight level FL250.

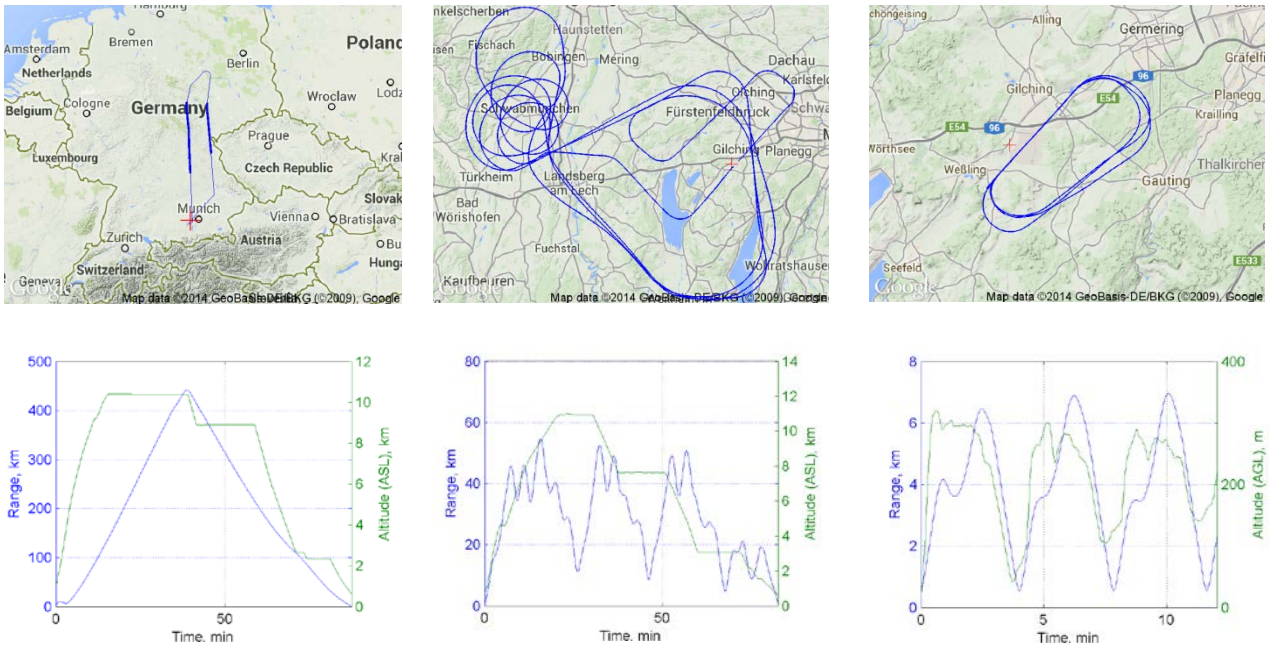

a) En-route flight

b) Enroute flight at different altitudes

c) Airport approach

Figure 4. Flight tracks as well as range and altitude for flights scenarios with 10MHz wide signals

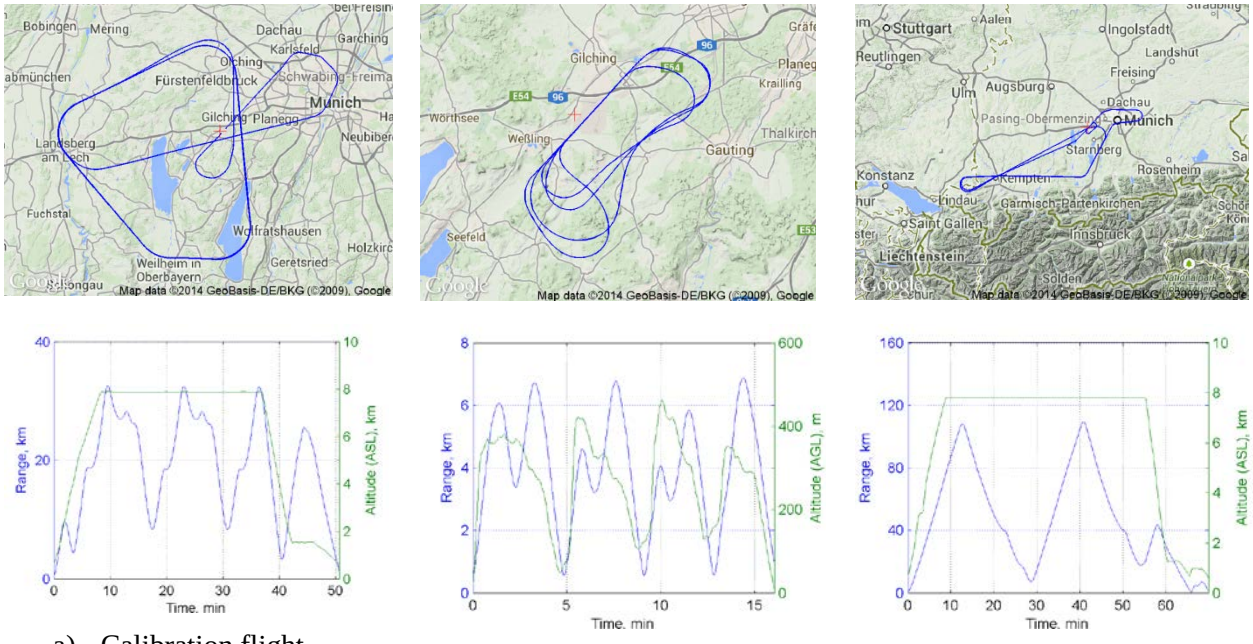

a) Calibration flight (Flight I)

b) Airport approach (Flight II)

c) In-band DME interference (Flight III)

Figure 5. Flight tracks as well as range and altitude for flights scenarios with 500kHz LDACS1 signals

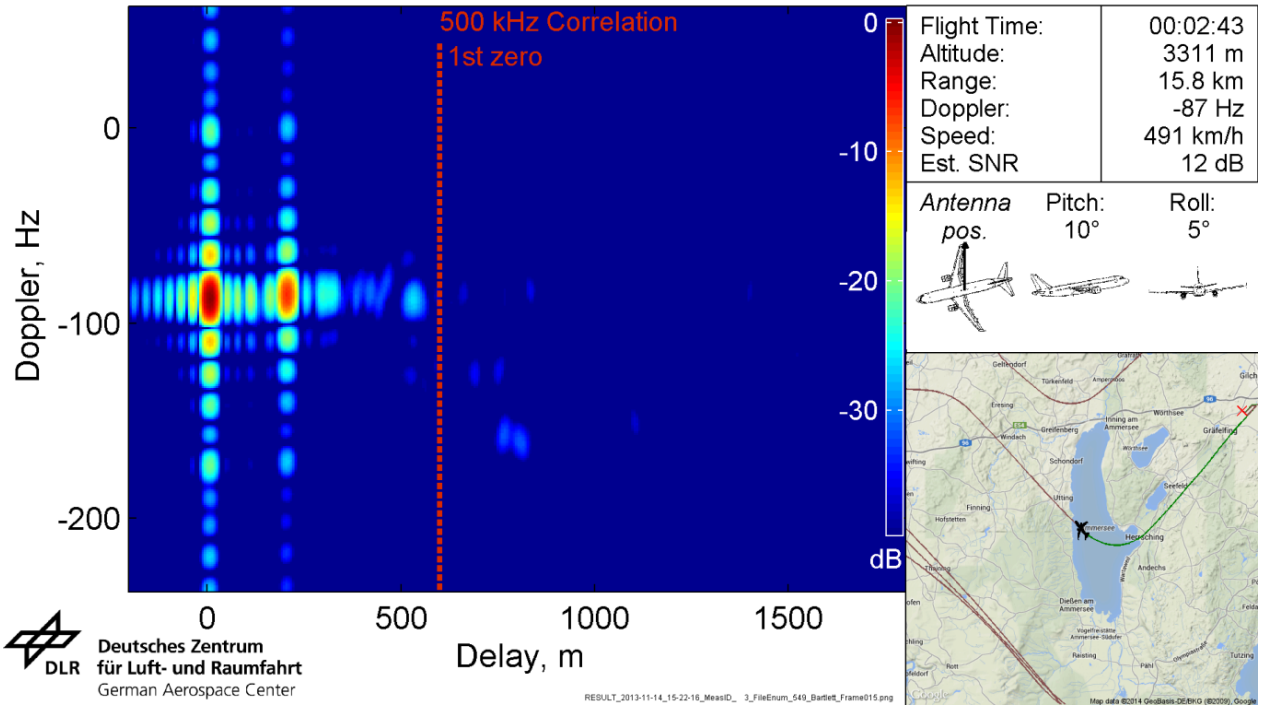

Figure 6. Estimated scatter function exhibiting a strong multipath interference

Multipath interference and its mitigation

The 10MHz-wide signals provide quite accurate information about the propagation environment. Using these signals it becomes possible to resolve individual propagation paths with delay differences exceeding 25-30 m without using superresolution techniques. In case of LDACS1 signals with the bandwidth of 500kHz this is possible for multipath generating excess delays of at least 500m. Thus, with wideband signals a conventional spectrogram (a Bartlett beamformer) can provide a relatively accurate characterization of the propagation environment.

Preliminary investigations of the collected measurement data demonstrate that the multipath interference might be severe in some cases. Results in Figure 6 show an example of such interference for a segment of a flight with 10MHz signal (the flight is shown in Figure 4b). It can be seen that the estimated scatter function indicates a presence of the second path. Its power is only 6 dB below the power of the line-of-sight (LOS), and the relative delay with respect to LOS is 209m; the Doppler shift with respect to LOS is insignificant and is estimated to be approx. 2Hz. It can be concluded that the second path originates in the vicinity of the transmitting antenna; it is most likely a reflection from a nearby building or airplane hangar. For signals with 500kHz bandwidth it will be very difficult to resolve such components in order to cancel the interference.

One of the possible approaches to mitigate multipath interference for ranging purposes is to smooth the "code-based" range estimate using Doppler information; in other words, a raw LDACS1 range estimate based on OFDM symbols can be smoothed using, e.g., a Hatch filter. This filter produces a smoothed estimate of the LDACS1 range $\hat{r}(t)$ as follows:

$$\hat{r}[n] = \alpha\, \tilde{r}[n] + (1-\alpha)\,(\hat{r}[n-1] - \lambda\, \widehat{f_D}[n] T_s), \quad (1)$$

where $\hat{r}[n]$ is a smoothed range estimate at the discrete time instance $n = \frac{t}{T_s}$, T_s is a sampling time, $\tilde{r}[n]$ is the corresponding "raw" (non-smoothed) LDACS1 range estimate, λ is the carrier wavelength,

$\widehat{f_D}[n]$ is an estimate of the Doppler shift, and α is a smoothing time constant of the Hatch filter. Such smoothing effectively "averages out" the impact of intermittent multipath. Obviously, the more persistent a multipath is, i.e., the longer the multipath is interfering with LOS, the more smoothing (smaller α) is necessary to reduce its effect.

Let us now show what impact Doppler smoothing has on ranging performance for LDACS1 signals. We will consider two ranging algorithms. The first will employ standard maximum likelihood (ML) algorithm to estimate raw range and Doppler frequency (see [8] and [9] for the details of the estimation algorithm). The ML algorithm is a simple snapshot-based optimization scheme that estimates delay and Doppler frequency of the measured signals. The other algorithm exploits particle filter (PF) for range estimation [10]. In contrast to the ML algorithm, the PF considers dynamics of the parameter estimates to optimize the estimator. This has an additional "smoothing" effect on the obtained estimates. The details of particle filter algorithm for range estimation can be found in [11].

Doppler–smoothed range estimation for LDACS1 signals

In the following we will demonstrate the impact of Doppler smoothing on the estimated range for three flights with LDACS1 signals: Flight I, a calibration flight (Figure 5a), Flight II, the airport approach flight (Figure 5b), and Flight III, the in-band DME interference flight (Figure 5c) with 0.5MHz separation between the DME and LDACS1 channels. We will study the ranging performance by computing the error between the LDACS1-based range estimates and those obtained using GPS coordinates of the airplane as follows: $e(t) = \hat{r}_{LDACS}(t) - \hat{r}_{GPS}(t)$. The delays of the signals caused by troposphere will not be taken into account in this work.

We will begin with the flight I. In this scenario, the measured signals exhibit quite mild multipath interference. The major disturbances are caused by aircraft banking, rather than multipath propagation. In the Figure 7 we show the estimated range error and the Doppler frequency of this scenario obtained using the ML and PF algorithms. What we immediately notice is that the ML algorithm tends to have a slightly higher estimation error, both in range,

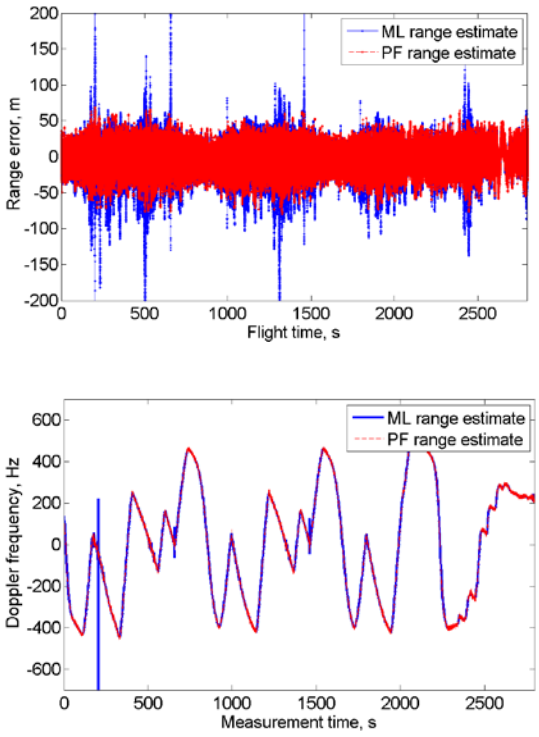

Figure 7. (a) Estimated range error and (b) estimated Doppler frequency for Flight I

as well as in Doppler. PF algorithm, on the other hand, performs better as it is able to smooth-out impulse like disturbances, especially for Doppler estimation results, which have a significant impact on the performance of the carrier smoothing filter. Now, let us look at the impact of carrier smoothing on the estimated range. To this end we consider the empirical distributions of the ranging error for 3sec and 12 sec smoothing. The corresponding plots, overlaid with that obtained for a non-smoothed range, are summarized in Figure 8.

What we see is that the width of the error distribution shrinks significantly. In the Table 2 we summarize the statistics (the mean range error and its standard deviation) of the obtained range errors. As we can see, the performance of the PF algorithm without smoothing outperforms ML algorithm: the variance of the estimated range error reduces by almost a factor of 4 for the PF algorithm. However, the use of carrier smoothing makes the difference between the algorithms marginal. Note that the bias of the estimators is only insignificantly affected by smoothing. The main contribution to the bias is due

to the tropospheric delays, not accounted by the estimator.

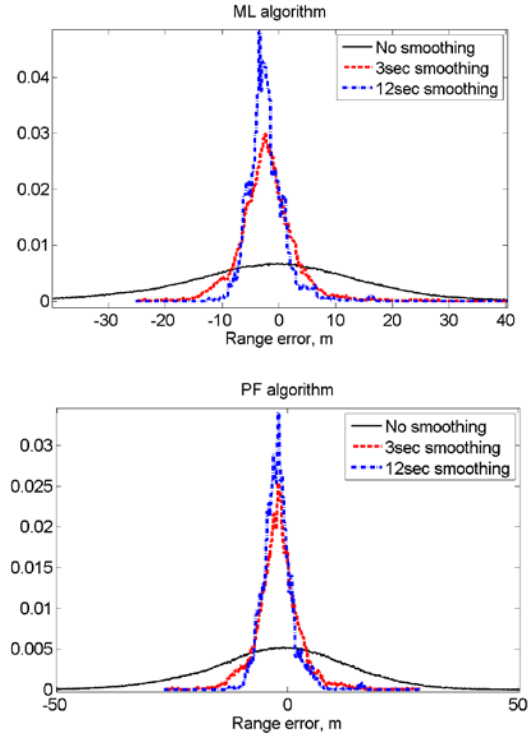

Figure 8. Flight I: histograms of range error for 3sec and 12sec smoothing for a) ML and b) PF algorithms

Table 2. Ranging error statistics for the Flight I

Algorithm	No smoothing	3sec	12sec
ML	-2,1m ±34.0m	-2,1m ±5.6m	-2.3m ±4.0m
PF	-1,9m ±15.64m	-2,0m ±5.4m	-2.2m ±3.9m

Now, let is look at the Flight II, airport approach flight (Figure 5b). As we see in Figure 9, this scenario is much more affected by multipath propagation. Notice that the range results obtained with the ML algorithm have impulse-like outliers, which are due to multipath interference. PF algorithm is more immune to these outbreaks due to its tracking ability. The error histograms in Figure 10 and range error statistics in Table 3 show a more detailed picture.

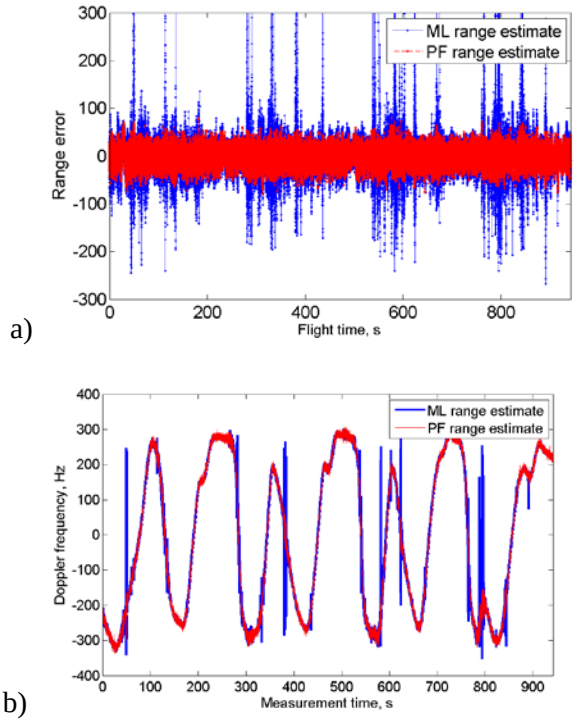

Figure 9. (a) Estimated range error and (b) Doppler frequency for Flight II

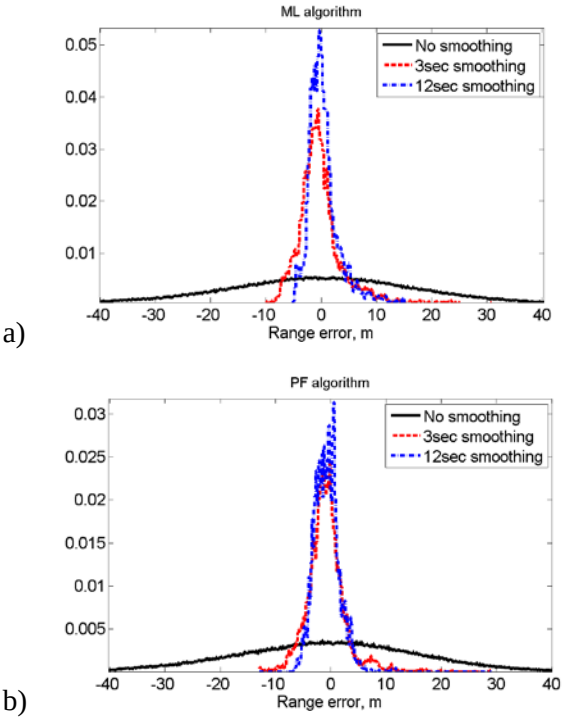

Figure 10. Flight II: histograms of range error for 3sec and 12sec smoothing for a) ML and b) PF algorithms

Table 3. Ranging error statistics for the Flight II

Algorithm	No smoothing	3sec	12sec
ML	+0.8m ±45m	0.7m ±6.9m	0.4m ±3.1m
PF	-0,8m ±17.3m	-0.7m ±3.8m	-0.7m ±2.3m

We see that the ML is positively biased, as compared to the PF algorithm. We also see that compared to the previous scenario the bias of the estimates is reduced. This can be explained by a reduced effect of the troposphere as the distance between the transmitter and receiver is smaller. For the Flight I this effect is more profound.

Finally, we consider the third flight (Figure 5c) with in-band DME interference. In Figure 11 we show a snapshot of the measured LDACS1 signal, sampled at 1.25MHz rate.

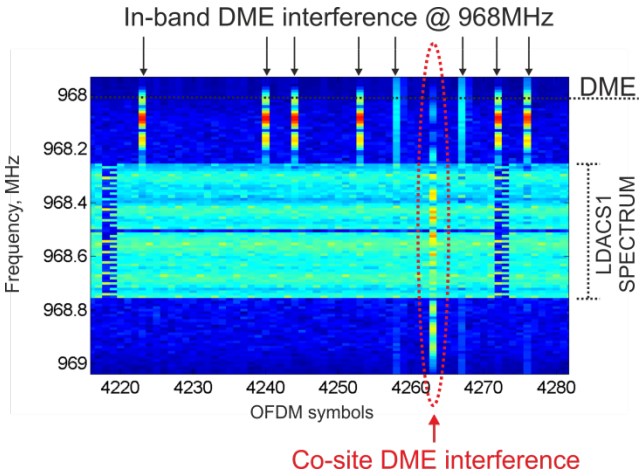

Figure 11. A snapshot of the measured signal spectrum for Flight III with in-band DME interference

We see that the interference from the DME ground station is clearly visible. The main impulse is, however, attenuated by the antialiasing filter. We can also clearly see the distinction between the DME interference caused by the ground DME station transmitting in the neighboring channel and that of the onboard DME transponder; the latter causes a co-site DME interference. The co-site interference is essentially a wideband disturbance that affects the LDACS channel bandwidth. In contrast, the pulse from the ground transmitter mainly affects the nearest frequencies. Now, let us consider the corresponding ranging results. Let us point out that this signal is affected not only by DME interference but also by multipath propagation, yet not as severely as the flight 2 (airport approach). In Figure 12 we demonstrate the investigated segment of the flight III. This segment corresponds to a part of the measurement with LDACS1 signal being only 0.5MHz away from the DME carrier frequency. The corresponding ranging results are summarized in Figure 13.

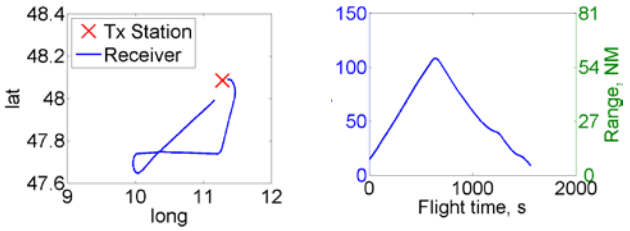

Figure 12. The investigated part of the Flight III with in-band DME interference at 968MHz and LDACS1 signal at 968.5MHz

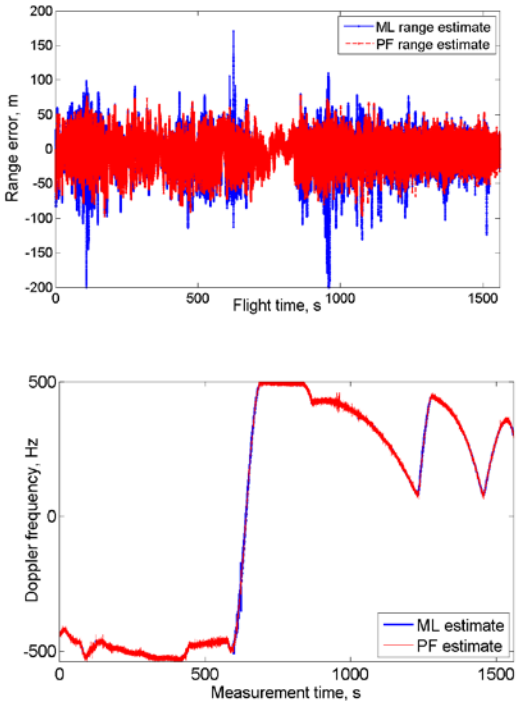

Figure 13. (a) Estimated range error and (b) Doppler frequency for Flight III

Here we observe a similar performance of the ranging algorithms we observed in previous cases. ML algorithm is more susceptible to interferences due to its snapshot-based nature. Also, we see that the in-band DME interference does not have a significant impact on the ranging performance. The analysis of the range error histograms shown in Figure 14 and the corresponding statistics in Table 4 supports this claim. We do see that the error distribution variance has increased, which can be due to the DME interference. However, we stress that for APNT purposes the performance loss of the ranging is insignificant. Note also that the PF algorithm outperforms ML scheme in case when no smoothing is applied. Using Doppler smoothing, however, levels the performance of both schemes; the performance differences become only marginal. Let us also indicate that for this flight the bias is the highest among the tested scenarios. This can be explained by the higher impact of the troposphere on the estimated range.

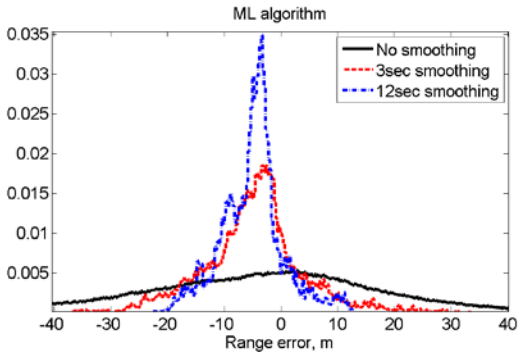

a)

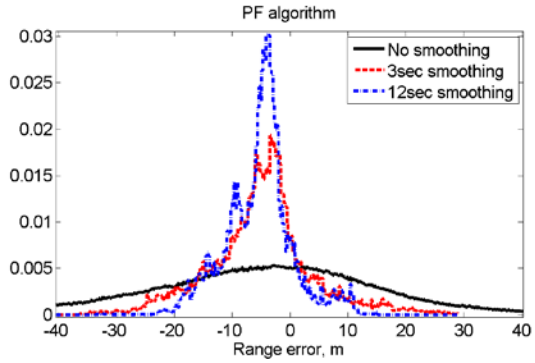

b)

Figure 14. Flight III: histograms of range error for 3sec and 12sec smoothing for a) ML and b) PF algorithms

Table 4. Ranging error statistics for the Flight III

Algorithm	No smoothing	3sec	12sec
ML	-4.8m ±26m	-4.9m ±10.4m	-5m ±7.5m
PF	-4.9m ±20.8m	-5.1m ±10.4m	-5.2m ±7.9m

Conclusions

This paper gives a short overview of the second flight measurement campaign initiated by the German Aerospace Center (DLR) with the aim to assess the LDACS1-based proposal for the APNT in more diverse scenarios as well as investigate the impact of multipath propagation on ranging performance for future ground-based APNT. In contrast to the measurements performed by DLR in 2012, the second measurement campaign includes only a single transmitter and an airborne receiver. In addition to LDACS1 signals, measurements with 10MHz signals were also performed. The latter permits a more detailed analysis of the propagation channel, specifically for ground-based APNT applications in L-band.

It has been previously identified that multipath might represent the major performance-limiting factor for APNT. As a possible countermeasure a Doppler smoothing has been applied and analyzed. Doppler-based range smoothing is an important technique that can significantly improve ranging performance of a ground-based ranging system: It provides a computationally simple way to mitigate or reduce intermittent multipath interference. However, persistent multipath components having small relative Doppler shifts might require larger smoothing intervals and reduce the performance of the smoothing filter. The severity and frequency of such cases is to be investigated using new 10MHz wideband measurement data.

Three flight scenarios have been analyzed in this work: a simple flight, which models an en-route scenario, an approach on the airport, where LDACS signals were measured at very low altitudes, and a scenario with in-band DME interference that closely mimics the future in-lay LDACS1 deployment scenario. Two algorithms have been investigated: a snapshot-based maximum likelihood estimator and a

particle filter based estimator. Both algorithms estimate range and Doppler frequency using measured signals. In all cases Doppler smoothing can significantly improve the ranging error, significantly reducing the standard deviation of the estimated range. However, the overly long smoothing might have an adverse effect by increasing range error bias. Smoothing constants up to 12 seconds were found to be sufficient for the considered scenarios. Once the smoothing is used the difference between maximum likelihood estimator and particle filter algorithm become insignificant.

Acknowledgments

The authors would like to thank the entire Institute of Communication and Navigation and the Institute of Flight Experiments at DLR for their continuous help, support and guidance during the realization of the measurement campaign. We are especially grateful for the great work of Boubeker Belabbas, Heinrich Brockstieger, Mihaela-Simona Circiu, Stefan Drumm, Bernhard Elwischger, Ulrich Epple, Uwe-Carsten Fiebig, Johann Furthner, Christian Gentner, Stefan Grillenbeck, Christoph Günther, Martin Hammer, Christian Hauswurz, Achim Hornbostel, Simon Kohn, Christian Mallaun, Ilaria Martini, Michael Meurer, Mohamad Mostafa, Werner Rox, Alexander Steingass, Matthias Süss, Robert Uebelacker, Wie Wang, and David Woudsma. Thanks also go to TimeTech GmbH, Stuttgart, for their rapid provision of measurement equipment and Rücker Aerospace GmbH, Oberpfaffenhofen, for their support during the aircraft certification process. We are also grateful for the help of Thomas Frank and Ken Tobler of National Instruments Germany in setting up the data acquisition equipment.

References

[1] EUROCONTROL, “The LDACS1 Prototype Specifications (D3 Deliverable),” BRUSSELS, 2009.

[2] D. Shutin, N. Schneckenburger, and M. Schnell, “LDACS1 for APNT — Planning and realization of a flight measurement campaign,” in *IEEE/AIAA 31st Digital Avionics Systems Conference (DASC)*, 2012.

[3] N. Schneckenburger, D. Shutin, and M. Schnell, “Precise aeronautical ground based navigation using LDACS1,” in *Integrated Communications Navigation and Surveillance Conference (ICNS)*, 2012.

[4] S. Naerlich, M. Schnell, and D. Shutin, “APNT – A New Approach Using LDACS1,” in *ICAO Navigation Systems Panel (NSP), Working Group of the Whole*, 2011.

[5] D. Shutin, N. Schneckenburger, M. Walter, and M. Schnell, “LDACS1 Ranging Performance - An Analysis of Flight Measurement Results,” in *Proc. of 32nd IEEE/AIAA Digital Avionics Systems Conference (DASC),*, 2013, pp. 3C6–1 – 3C6–10.

[6] Reiner S. Thomä, M. Landmann, A. Richter, and U. Trautwein, “Smart Antennas - State of the Art,” in *EURASIP Book Series on SP&C*, Hindawi Publishing Corporation, 2005, pp. 241–270.

[7] S. Naerlich, D. Shutin, and S. Michael, “The LDACS-NAV Project,” in *ICAO Navigation Systems Panel (NSP), Working Group of the Whole*, 2012.

[8] S. Kay, *Fundamentals of Statistical Signal Processing, Volume I: Estimation Theory (v. 1)*. Prentice Hall, 1993, p. 625.

[9] D. Shutin, W. Wang, and T. Jost, “Incremental Sparse Bayesian Learning for Parameter Estimation of Superimposed Signals,” in *10th International Conference on Sampling Theory and Applications*, 2013.

[10] B. Ristic, S. Arulampalam, and N. Gordon, *Beyond the Kalman Filter: Particle Filters for Tracking Applications*. Artech House, 2003.

[11] T. Thiasiriphet, N. Schneckenburger, and D. Shutin, “Application of Bayesian Filtering for Multipath Mitigation in LDACS1-based APNT Applications,” in *ION GNSS+ , to appear*, 2014.